ACS APPLIED MATERIALS & INTERFACES

Research Article

www.acsami.org

One-Step Synthesis of Robust Amine- and Vinyl-Capped Magnetic Iron Oxide Nanoparticles for Polymer Grafting, Dye Adsorption, and Catalysis

Li Zhou,* Benzhao He, and Jiachang Huang

Key Laboratory of New Processing Technology for Nonferrous Metal and Materials (Ministry of Education), Guangxi Scientific Experiment Center of Mining, Metallurgy and Environment, and College of Material Science and Engineering, Guilin University of Technology, Guilin 541004, Guangxi, China

Supporting Information

ABSTRACT: Magnetic iron oxide nanoparticles (MIONs) bearing amine and vinyl groups are fabricated straightforwardly using vinyl-based tertiary amine molecules as both alkaline source and ligands based on the coprecipitation of iron ions in aqueous solution. The as-prepared MIONs present amphiphilic performance that can be well-dispersed both in aqueous solution and common organic solvents (e.g., ethanol, dichloromethane and tetrahydrofuran). Transmission electron microscopy (TEM), X-ray diffraction (XRD), and vibrating sample magnetometer (VSM) measurements reveal that the MIONs are superparamagnetic Fe_3O_4 nanoparticles with a mean diameter below 10 nm. The presence of ligands on the surface of MIONs was confirmed by thermogravimetric analysis (TGA), Fourier transform infrared (FTIR), and X-ray photoelectron spectroscopy (XPS) characterizations. Benefiting from the surface vinyl groups, the MIONs are able to graft polyvinyl-based polymers by in situ polymerization of the corresponding vinyl monomers as confirmed by grafting poly(methyl methacrylate) (PMMA) in this paper. On the basis of their surface amine groups, the MIONs show high adsorption capacity (ca. 0.42 mmol/g) for congo red dye and excellent performance for in situ growth of Pt nanocatalyst. Moreover, the MIONs possess high stability and can be reused several times without obvious decrease of their adsorption capacity and catalytic efficiency. Considering the facile fabrication process and versatile performance of the obtained MIONs, this work may open up new opportunities for the large-scale applications of MIONs.

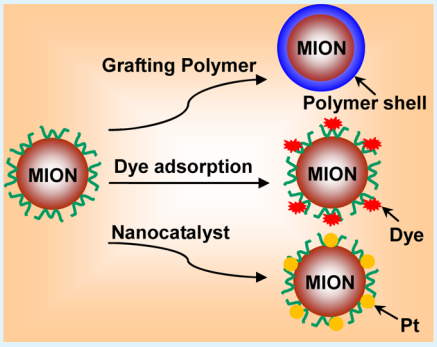

KEYWORDS: *magnetic iron oxide, nanoparticles, polymer grafting, dye adsorption, catalysis*

1. INTRODUCTION

Over the past few decades, magnetic iron oxide nanoparticles (MIONs) have attracted intense attention due to their potential applications in a wide range of areas, including catalysis, data storage, sensing, magnetic resonance imaging, drug delivery, and environmental remediation.[1−6] For all these applications, MIONs with favorable surface functionality and facile availability are pursued.

There are two common strategies to synthesize MIONs. One is based on the decomposition of organic iron precursors (e.g., $Fe(CO)_5$ and iron(III) acetylacetonate) at high temperature in nonpolar organic solvents.[7−9] By this strategy, MIONs with controllable size and narrow size distribution can be easily synthesized.[10,11] However, these MIONs cannot be directly applied in biosystems due to their hydrophobic surfaces. Alternatively, water-dispersible MIONs can be fabricated at various scales in aqueous solution by precipitating iron ions in alkaline solutions (e.g., NaOH and $NH_3{\cdot}H_2O$).[12,13] In order to obtain a stable MION dispersion in water, hydrophilic organic ligands including functional small molecules (e.g., β-cyclodextrin and sucrose)[14,15] and polymers (e.g., polyvinylpyrrolidone, polyvinyl alcohol, poly(acrylic acid), and hyperbranched polyglycerol)[16−19] are generally required during the reaction processes. Though numerous MIONs have been reported, MIONs with high dispersibility in both water and common organic solvents has rarely been reported. As the proposed applications need to process MIONs in diverse solvents, a lack of an efficient approach to prepare processable MIONs in large quantities would be a major obstacle for large-scale application of MIONs.

On the other hand, a number of applications (e.g., energy storage devices, microwave absorbers, and electronics) need to embed the MIONs into polymer matrix to form magnetic polymer nanocomposites (MPNs).[20−22] A major challenge for preparing high performance MPNs is the serious aggregation of MIONs in polymer matrix because of the poor interface compatibility between the MION phase and the polymer phase.[23] Though this challenge can be overcome through tailoring the surface of MIONs, additional reaction steps greatly restrict the progress of MPNs since most of the current MPNs

Received: June 16, 2013
Accepted: August 12, 2013
Published: August 12, 2013

are directly fabricated from the as-prepared MIONs.[23] A possible approach to simplify the procedure of fabricating MPNs is to achieve one-step synthesis of versatile MIONs, which can be grafted with polymers by in situ polymerization or can be well-dispersed in various solvents for direct blending with polymers.

Recently, organic amine molecules as both alkaline source and ligand for synthesis of water-dispersible MIONs have been reported.[24−27] A variety of amine molecules such as 1,6-hexanediamine, di-*n*-propylamine, ethanediamine, and tetramethylammonium hydroxide were chosen to prepare MIONs.[24−27] Inspired by these results, we expect that the ligands, containing both amine group and vinyl group, may lead to formation of MIONs with high dispersibility in both aqueous solution and organic solvents. To the best of our knowledge, one-step synthesis of amine- and vinyl-capped MIONs with amphiphilic performance has not been reported.

In this contribution, we present a facile and effective approach to produce amine- and vinyl-capped MIONs by employing vinyl-based tertiary amine molecules as both alkaline source and ligands (Scheme 1). This synthetic protocol shows

Scheme 1. Cartoon Illustration for the Structure of Amine- and Vinyl-Capped MION (Left) and the Chemical Structures of the Used Ligands (Right)

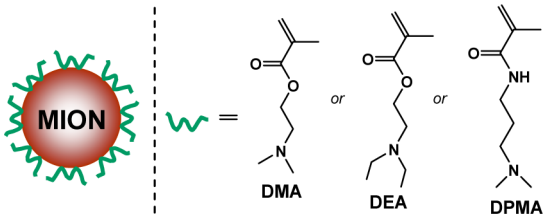

remarkably combined merits as follows: (1) the amine and vinyl groups of the ligand endow the MIONs with high dispersibility both in water and organic solvents and, thus, can offer good processability for various applications; (2) the vinyl groups allow further modifications (e.g., in situ grafting polymers); (3) the amine groups can be used to adsorb anionic organic molecules or complex metal ions; and moreover (4) the MIONs can be produced by a simple one-step reaction, which is highly desired for practical applications. Postfunctionalization investigations reveal that the MIONs are able to graft polymer by in situ radical polymerization of vinyl monomers based on their surface vinyl groups. Further dye adsorption and catalysis studies demonstrate that the MIONs can serve as a promising magnetic adsorbent for the removal of anionic dye and as a magnetic support for in situ growth of highly efficient noble metal nanocatalyst, respectively.

2. EXPERIMENTAL SECTION

Materials. Iron(III) chloride ($FeCl_3$) powder, iron(II) chloride tetrahydrate ($FeCl_2{\cdot}4H_2O$), 2-(dimethylamino)ethyl methacrylate (DMA, 99%), 2-(diethylamino)ethyl methacrylate (DEA, 99%), *N*-[3-(dimethylamino)propyl] methacrylamide (DPMA, 99%), ammonia solution (25 wt %), azobisisobutyronitrile (AIBN), methyl methacrylate (MMA), congo red (CR), methylene blue (MB), potassium tetrachloroplatinate (K_2PtCl_4), 4-nitrophenol, and sodium borohydride ($NaBH_4$) were purchased from Aladdin Chemistry Co. Ltd. (Shanghai, China). DMA, DEA, DPMA, and MMA were further purified by passing a column of alumina. AIBN was employed after twice recrystallization. All other reagents were used as received without further purification.

Characterization. Fourier transform infrared (FTIR) spectra were measured on a Thermo Nexus 470 FT-IR spectrometer (KBr disk). Thermogravimetric analysis (TGA) was carried on a TGA Q500 analyzer with a heating rate of 20 °C min^{-1} in nitrogen flow. Transmission electron microscope (TEM) and energy disperse spectroscopy (EDS) studies were performed on a JEOL-2010 TEM at 200 kV. X-ray powder diffraction (XRD) spectra were taken on a Holland PANalytical X-Pert PRO X-ray diffractometer with Cu Kα radiation. The magnetic moment was recorded at 300 K on a MPMS XL-7 vibrating sample magnetometer (VSM). X-ray photoelectron spectroscopy (XPS) measurements were made on Kratos AXIS UltraDLD (Kratos Analytical Ltd.) with mono Al Kα radiation ($h\nu$ = 1487.71 eV) at a power of 75 W. Absorption spectra were recorded on a UV-3600 UV−vis spectrophotometer (Shimadzu).

One-Step Synthesis of Amine- and Vinyl-Capped MIONs. The MIONs synthesized by using DMA, DEA, and DPMA as alkaline source are named MION-DMA, MION-DEA, and MION-DPMA, respectively. In a typical procedure, 162 mg of $FeCl_3$ (1 mmol) and 99 mg of $FeCl_2{\cdot}4H_2O$ (0.5 mmol) were added into 50 mL of deionized water with mechanical stirring to completely dissolve the iron salts. Subsequently, 6 mmol of DMA (or DEA, DPMA) was added to the mixture. The mixture was stirred for another 30 min at 80 °C. Finally, the resulted MIONs were collected by centrifugation at 12 000 rpm/min for 5 min and washed several times with water and ethanol. The product was dried under vacuum at 50 °C for 12 h, obtaining 124.8 mg of MION-DMA (or 130.5 mg of MION-DEA, 126.3 mg of MION-DPMA). For comparison, MION-$NH_3{\cdot}H_2O$ nanoparticles were synthesized by using $NH_3{\cdot}H_2O$ instead of organic ligands as alkaline source by keeping other parameters constant during the synthetic process.

TGA data between 100 and 700 °C: 7.2, 11.2, 8.3, and 1.6 wt % for MION-DMA, MION-DEA, MION-DPMA, and MION-$NH_3{\cdot}H_2O$, respectively. The density of organic ligands (mmol/g) per gram of MIONs was calculated according to the following formula:

$$\text{density of organic ligands} = 1000 f_{wt}/M_{ol}$$

where f_{wt} is the weight fraction of capped organic ligand calculated from the corresponding TGA data between 100 and 700 °C, M_{ol} (g/mol) is the molar mass of organic ligand. Correspondingly, the densities of DMA, DEA, and DPMA for their corresponding MIONs are calculated as ca. 0.458, 0.605, and 0.488 mmol/g, respectively.

Synthesis of MION-*g*-PMMA [Poly(methyl methacrylate)]. A typical procedure is given as follows: 20 mg of MION-DMA dispersed in 15 mL of *N*,*N*-dimethylformamide (DMF) was added to 50 mL flask and was sonicated in a 40 kHz sonic bath for 10 min followed by introducing 20 mmol of MMA monomer. Under argon flow protection and vigorous mechanical stirring, 0.1 mmol of AIBN was added. The flask was then immersed in a 65 °C oil bath. After 48 h, 30 mL of dichloromethane was added. The black solids were collected by centrifugation and washed with dichloromethane for several times. Finally, the product was dried in a vacuum oven at 35 °C for 12 h, yielding 26.6 mg of MION-*g*-PMMA.

Adsorption of Dye. CR and MB as typical dyes were chosen for adsorption experiments. Typically, 20 mg of magnetic adsorbent (MION-DMA or MION-$NH_3{\cdot}H_2O$) was mixed with 4 mL of known concentration of dye solution at 20 °C. The solution pH was adjusted by NaOH (0.1 M) or HCl (0.1 M). The mixture was stirred at 100 rpm at 20 °C. The samples were withdrawn from the experimental flask at predetermined time interval until adsorption equilibrium was achieved. The magnetic adsorbent was collected by a magnet. The residual dye concentration was determined by UV−vis spectroscopy by measuring the absorbance at a wavelength of maximum absorbance. It should be pointed that the absorption curves of CR solution in the pH range 7−11 are different from the curves in the pH range 4−6. Calibration curves were plotted between absorbance and concentration of the standard dye solutions at different pH values. All adsorption experiments were carried out in triplicate, and the average values were used to minimize random error. The effect of pH on the amount of dye adsorption was analyzed in the pH range 4−11.

Adsorbent Regeneration. For the dye desorption, typically, 20 mg of CR-adsorbed MION-DMA was added to 4 mL of aqueous solution at pH 11, and the suspension was stirred for 2 h. Finally, the MION-DMA adsorbent was collected by a magnet and reused for adsorption again. The supernatant solution was analyzed by UV−vis spectroscopy. The cycles of desorption−adsorption processes were successively conducted five times.

Synthesis of Magnetic MION-Pt Nanocatalyst. Typically, 10 mg of K_2PtCl_4 (0.024 mmol) aqueous solution and MION-DMA (30 mg) was mixed in 4 mL of deionized water and stirred at room temperature for 24 h. After that, the solid was separated by a magnet and washed with deionized water. This magnetic separation and wash process was repeated three times, and 0.1 mL of freshly prepared $NaBH_4$ (0.1 M) aqueous solution was added and stirred for 30 min. After repeatedly being washed by water, the resulting solid was dried overnight in a vacuum, yielding 30.7 mg of MION-Pt.

Reduction of 4-Nitrophenol by MION-Pt Catalyst. Typically, in a standard quartz cuvette, 4-nitrophenol (0.04 mL, 0.01 M), $NaBH_4$ (0.1 mL, 0.1 M), and deionized water (2.5 mL) were added. After addition of MION-Pt catalyst (6 mg), the mixture was agitated by using a small glass stirring rod. The bright yellow solution gradually faded as the reaction progressed. UV−vis spectra were monitored in the sequence of time. After the catalytic reaction, the MION-Pt was collected by a magnet and washed with ethanol. Then, the recovered catalyst was reused for the next cycle of catalysis. The same procedure was repeated ten times.

3. RESULTS AND DISCUSSION

Synthesis and Characterization. MIONs, containing amine and vinyl groups, can be fabricated in large quantities by using vinyl-based tertiary amine molecules as ligands under a mild condition. The reason for employing vinyl-based tertiary amine molecules as ligand is based on the following considerations. On one hand, the amine part of the ligand is able to act as alkaline source for formation of MIONs. On the other hand, the hydrophilic amine part associated with hydrophobic vinyl part can not only endows the MIONs with amphiphilic characteristic but also provides reactive platform for further modification. As illustrated in Scheme 1, 2-(dimethylamino)ethyl methacrylate (DMA), 2-(diethylamino)-ethyl methacrylate (DEA), and *N*-[3-(dimethylamino)propyl] methacrylamide (DPMA) were chosen as typical ligands in this study. The MIONs synthesized by using DMA, DEA, and DPMA as ligands are named MION-DMA, MION-DEA, and MION-DPMA, respectively. As expected, all MIONs show good dispersibility both in aqueous solution and organic solvents such as *N*,*N*-dimethylformamide (DMF), ethanol, dichloromethane (DCM), and tetrahydrofuran (THF) as presented in Figure 1.

The size and morphology of the synthesized MIONs were observed through transmission electron microscope (TEM) as shown in Figures 2a−c. All MIONs show irregularly spherical shapes with sizes in the range of 5−13 nm. The average diameters of MION-DMA, MION-DEA, and MION-DPMA by counting 100 particles are 8.2, 7.3, and 7.6 nm, respectively. The crystal lattice fringes of MIONs can be clearly seen in the corresponding high resolution TEM images (the inset), indicating that all MIONs are well-crystallized. The crystalline structures of MIONs were further identified by powder X-ray diffraction (XRD) (Figure 2d). The diffraction patterns and relatively intensities of all the peaks matched well with those of Fe_3O_4 (JCPDS 19-0629),[28] implying that the vinyl-based tertiary amine ligands are helpful to form Fe_3O_4 nanoparticles. Meanwhile, the magnetic properties of MIONs were measured by vibrating-sample magnetometer (VSM) at 300 K (Figure 2e). The magnetization curves show that all the samples are superparamagnetic at room temperature. The saturation magnetization values of MION-DMA, MION-DEA, and MION-DPMA are 28.5, 24.5, and 27.4 g/emu, respectively, indicating that all MIONs have strong magnetic responsibility to external magnetic field. In fact, the MIONs can be collected from aqueous dispersion within 30 s by using a magnet of 2000 Gs.

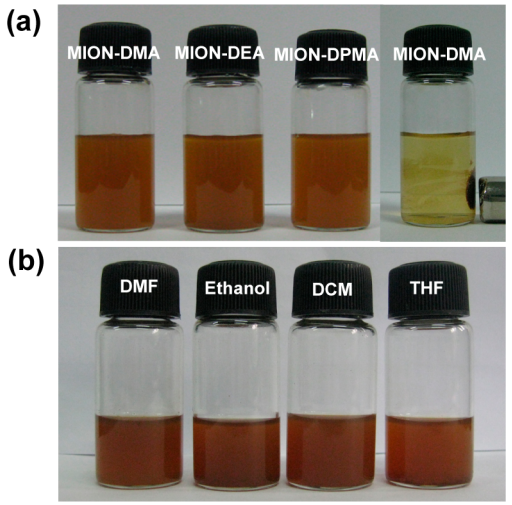

Figure 1. (a) Photographs of MION-DMA, MION-DEA, and MION-DPMA in aqueous solution and MION-DMA dispersion after placement of a magnet. (b) Photographs of MION-DMA in various organic solvents.

The contents of organic ligands on the surface of MIONs were determined by thermo gravimetric analysis (TGA) as depicted in Figure 3a. For comparison, MIONs by using ammonia as alkaline source (MION-$NH_3{\cdot}H_2O$) was also synthesized (see Figures S1 in the Supporting Information). The weight-losses of MION-DMA, MION-DEA, and MION-DPMA from 100 to 700 °C are ca. 7.2, 11.2, and 8.3 wt %, respectively, revealing that the ligands have been successfully capped onto the surface of MIONs. Correspondingly, the densities of DMA, DEA, and DPMA for their corresponding MIONs are calculated as ca. 0.458, 0.605, and 0.488 mmol/g, respectively. Such high content of organic component promises efficient reactive platform for further applications. While for MION-$NH_3{\cdot}H_2O$ sample, only ca. 1.6 wt % weight-loss from 100 to 700 °C is observed, which should be ascribed to the volatilization of the residue water in the sample. Figure 3b shows the Fourier transform infrared (FTIR) spectra of the as-prepared MIONs. A strong band at around 587 cm^{-1} corresponding to Fe−O vibration can be observed for all samples. Compared with MION-$NH_3{\cdot}H_2O$, the organic ligands-capped MIONs exhibit two bands at 2865 and 2930 cm^{-1} corresponding to C−H stretching. For MION-DMA and MION-DEA, two obvious bands at 1143 and 1725 cm^{-1} corresponding to C—O—C and C═O stretching, respectively, can be seen. In addition, the MION-DPMA sample shows a strong amide (II) band at 1542 cm^{-1}. All these FTIR results are well in accordance with the predicted structure. In order to gain more structure information, MION-DMA was chosen as a representative for X-ray photoelectron spectroscopy (XPS) measurement. According to the full survey spectrum (Figure 3c), the elements of Fe, O, N, and C are found, of which the elements of O, N, and C arise from the component of DMA.

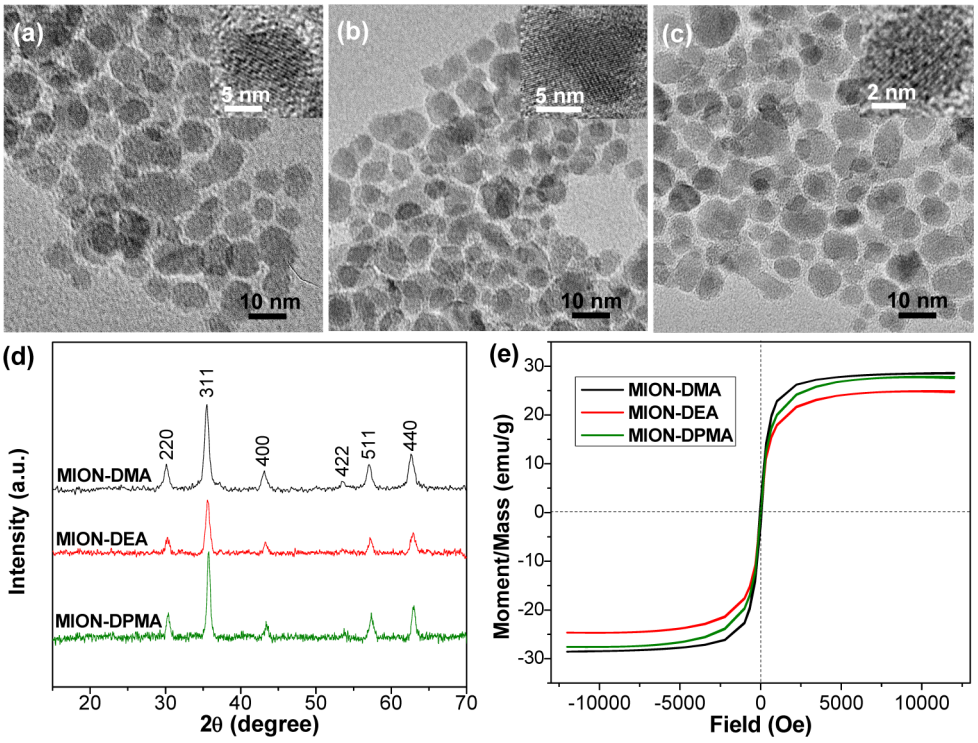

Figure 2. TEM images of (a) MION-DMA, (b) MION-DEA, and (c) MION-DPMA. (d) XRD patterns and (e) magnetization curves (at 300 K) of MION-DMA, MION-DEA, and MION-DPMA.

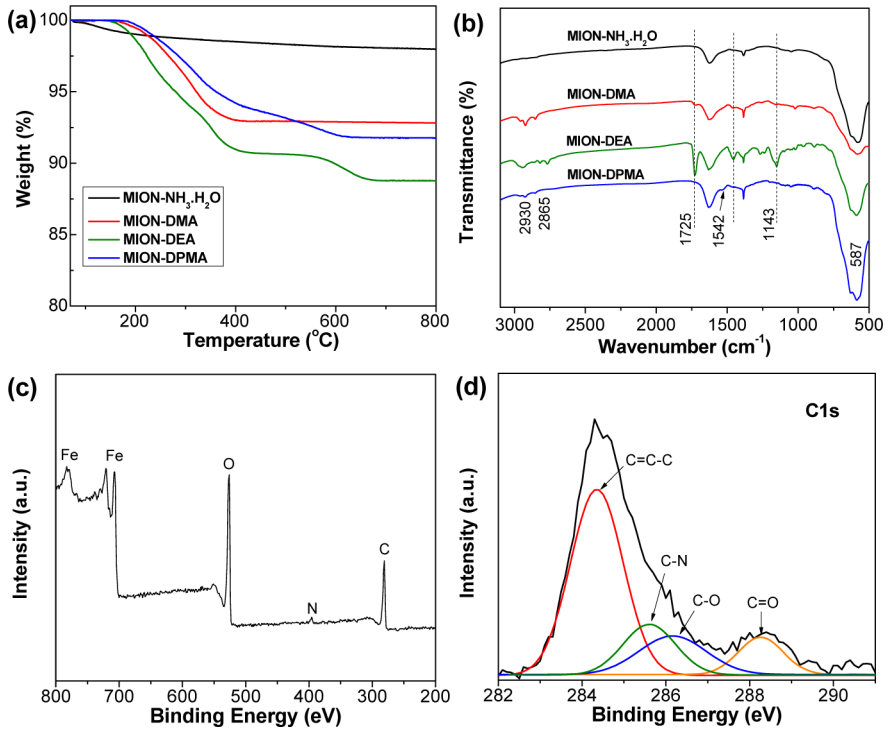

Figure 3. (a) TGA curves and (b) FTIR spectra of the synthesized MIONs. (c) XPS survey spectrum and (d) C 1s spectrum of MION-DMA.

Meanwhile, the atom ratio of C/N/O calculated from the XPS result is 8/1/2, which is in good agreement with the DMA molecule. Consistent with the FTIR result, the corresponding high-resolution C 1s spectrum in Figure 3d indicates that MION-DMA contains C—O, C═O, and C—N groups. On the basis of the above results, we can conclude that amine- and vinyl-capped MIONs with relatively uniform size, good superparamagnetic performance, and high dispersibility in both water and organic solvents can be facilely prepared by utilizing vinyl-based tertiary amine molecules as ligands.

Polymer Grafting. Recently, a new class of functional nanohybrid based on the combination of MION with polymer has attracted increasing attention due to its excellent properties for a variety of potential applications.[29−31] Since the as-

dx.doi.org/10.1021/am402334f | ACS Appl. Mater. Interfaces 2013, 5, 8678−8685

prepared MIONs possess multiple vinyl groups, it is expected that polyvinyl-based polymers could be grafted from the surface of MIONs through in situ radical polymerization of the corresponding vinyl monomers. In this work, we chose MION-DMA and methyl methacrylate (MMA) as a representative MION and vinyl monomer, respectively, to demonstrate the feasibility of polymer grafting. The final sample was characterized by TGA, FTIR, and TEM measurements. After grafting reaction, the weight-loss of the resulted MION-*g*-PMMA from 100 to 700 °C increased to 31.2 wt %, which is much higher than that of MION-DMA (7.2 wt %) (Figure 4a).

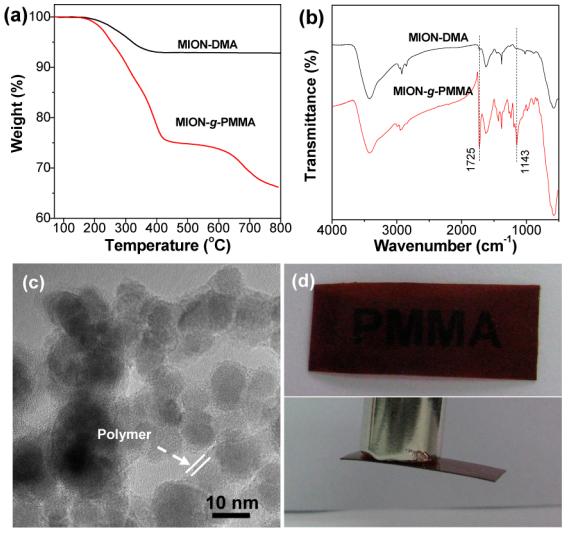

Figure 4. (a) TGA curves and (b) FTIR spectra of MION-DMA and MION-*g*-PMMA. (c) Representative TEM image of MION-*g*-PMMA. (d) Photographs of transparent magnetic MION-*g*-PMMA/PMMA film before (top) and after (bottom) placement of a magnet.

The high weight-loss demonstrated that PMMA has been grafted from the surface of MION-DMA. In the FTIR spectrum of MION-*g*-PMMA (Figure 4b), the two bands at 1143 and 1725 cm^{-1} corresponding to C—O—C and C═O stretching, respectively, become much stronger as compared with MION-DMA, further confirmed the successful grafting of PMMA. More direct evidence for the formation of MION-*g*-PMMA is shown in the TEM image (Figure 4c). As can be seen, an obvious polymer layer envelops the MION. It should be pointed that the MION-*g*-PMMA shows excellent dispersibility in organic solvents such as DCM and THF. On the basis of its good dispersibility, through simple blending of the as-prepared MION-*g*-PMMA with commercial PMMA (M_w 70 000) in DCM, followed by solvent evaporation, transparent magnetic MION-*g*-PMMA/PMMA nanocomposite film can be obtained (Figure 4d). Therefore, the obtained MIONs are quite robust for preparing magnetic nanohybrids or nanocomposites.

Dye Adsorption. Dyes are widely used in industrial fields such as textile, printing, paper-making, and food. It is estimated that 10−15% of the dyes are lost during the dyeing process and released as effluent.[32] Discharging of dyes into water even in a small amount can affect the aquatic life and food web. Therefore, the removal of dyes from effluent is of great importance. An efficient approach to remove dyes from wastewater is by adsorption technique. During the past decades, activated carbon (AC) is the most commonly used adsorbent. However, the AC suffers from some drawbacks such as difficult separation and regeneration. Recently, magnetic materials with high adsorption capacity and facile magnetic separation character are emerging as a new type of adsorbent.[33−35]

As the obtained MIONs possess numerous positively charged tertiary amine groups, we anticipate that they are able to adsorption of anionic dyes from aqueous solution. In this study, methylene blue (MB) as a typical cationic dye and congo red (CR) as a typical anionic dye (Figure 5a) were

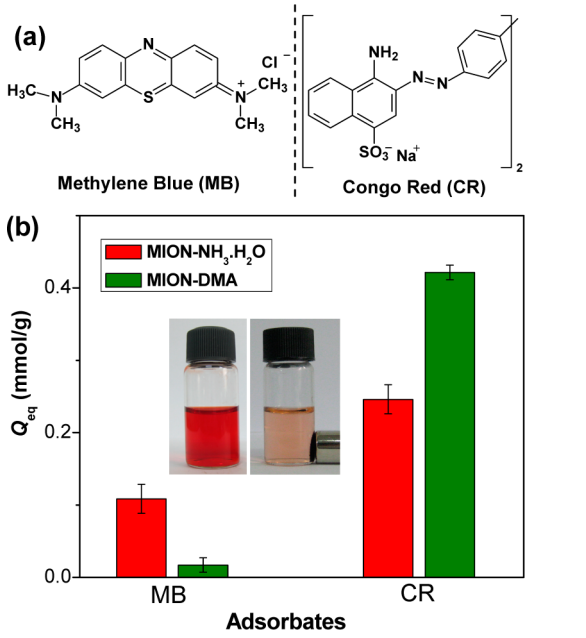

Figure 5. (a) Chemical structures of MB and CR. (b) Adsorption capacities of MION-NH_3·H_2O and MION-DMA for MB and CR dyes. The initial dye concentration is 5 mM. Inset shows photographs of CR solution before (left) and after (right) adsorption on MION-DMA.

chosen to test the adsorption performance of MION-DMA. The amount of dyes adsorbed at equilibrium was calculated from the following mass balance equation[35]

$$Q_{eq} = \frac{(C_0 - C_{eq})V}{m}$$

where Q_{eq} (mmol/g) is the amount adsorbed per gram of adsorbent at equilibrium, C_0 (mmol/L) is the initial concentration of dyes in the solution, C_{eq} (mmol/L) is the concentration of dyes at equilibrium, V (L) is the volume of the solution, and m (g) is the mass of the adsorbent used. The Q_{eq} of MION-DMA for CR reaches up to 0.42 mmol/g (Figure 5b). This value compares favorably to MION-NH_3·H_2O (0.24 mmol/g) and other reported adsorbents such as coal-based mesoporous activated carbons (0.22 mmol/g) and modified hectorite (0.28 mmol/g).[36,37] The inset of Figure 5b shows the aqueous solution of CR before and after adsorption on MION-DMA. After adding MION-DMA, the color of the CR solution significantly faded. Moreover, the adsorbent could be readily separated from water by a magnet. In contrast, the MION-DMA showed low Q_{eq} (0.02 mmol/g) for MB. On the basis of the Q_{eq} results, we speculate that the adsorption performance of MION-DMA is strongly dependent on the interactions between the positively charged amine groups of MION-DMA and the functional groups of dyes. Because the CR contains negatively charged $-SO_3^-$ group, the MION-DMA can efficiently adsorb it by strong electrostatic attraction. While

dx.doi.org/10.1021/am402334f | ACS Appl. Mater. Interfaces 2013, 5, 8678−8685

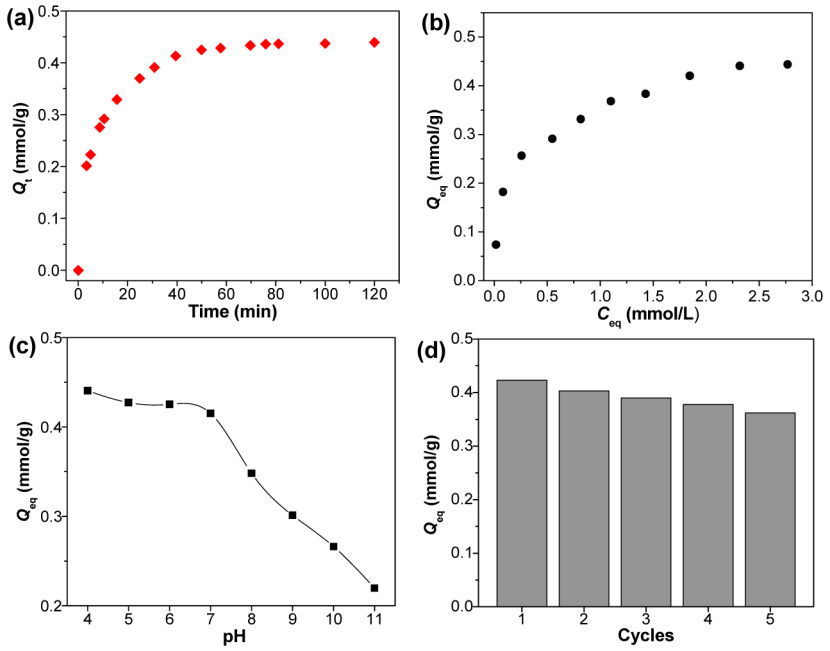

Figure 6. (a) Time profile of CR adsorption on MION-DMA (pH = 7.0). (b) Adsorption isotherm for the adsorption of CR on MION-DMA at pH 7.0 and 20 °C. (c) Effect of pH on the adsorption of CR on MION-DMA. (d) Adsorption capacity of MION-DMA in five successive cycles of desorption-adsorption. For a, c, and d, the initial CR concentration is 5 mM and the temperature is 20 °C.

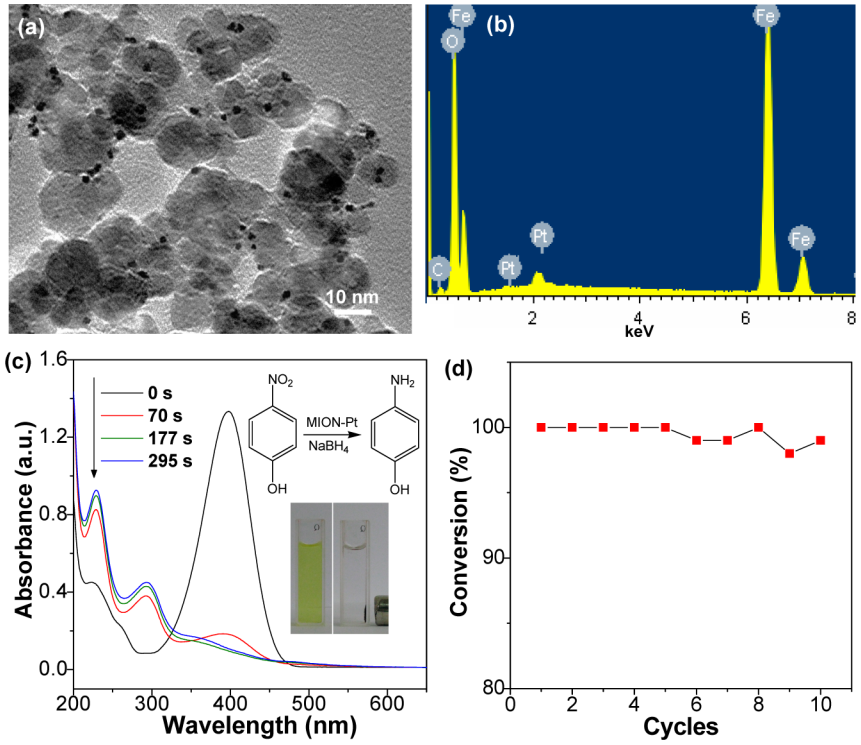

Figure 7. (a) Representative TEM image of MION-Pt. (b) EDS spectrum of MION-Pt shown in part a. (c) UV−vis spectra showing the gradual reduction of 4-nitrophenol with MION-Pt catalyst. The inset of part c shows the photographs of 4-nitrophenol and $NaBH_4$ solution before adding MION-Pt (left) and magnetic separation of MION-Pt after the reaction (right). (d) Conversion of 4-nitrophenol in ten successive cycles of reduction and magnetic separation with MION-Pt catalyst.

for MB, it possesses positively charged $-N^+$ group. The electrostatic attraction between MB and MION-DMA is very weak. Therefore, the MION-DMA adsorbent is suitable for adsorption of anionic dyes or other negatively charged molecules.

For practical adsorption applications, the contact time required to reach adsorption equilibrium is an important parameter for adsorbent. The effect of the contact time on the adsorption of CR by MION-DMA is presented in Figure 6a. As can be seen, the adsorption process reaches equilibrium in about 45 min, indicated rapid adsorption rate of the MION-

dx.doi.org/10.1021/am402334f | ACS Appl. Mater. Interfaces 2013, 5, 8678−8685

DMA. To study the adsorption mechanism, the relationship between the amount of CR adsorbed and the CR concentration remaining in solution is described in Figure 6b. The equilibrium adsorption data were analyzed by the well-known Langmuir and Freundlich isotherm models (for details, see Table S1 and Figures S2 and S3 in the Supporting Information). The results reveal that the Langmuir model fits better than Freundlich model to the experimental adsorption data. In addition, the effect of pH on the adsorption of CR on MION-DMA was investigated (Figure 6c). The solution pH would affect both aqueous chemistry and surface binding-sites of the adsorbent. The Q_{eq} decreased obviously with increasing pH from 7 to 11 and slightly decreased with increasing pH from 4 to 7. At high pH, excessive hydroxyl ions might compete with the dye anions and hence obvious reductions in dye uptake were observed. On the other hand, this result implies that the adsorbed MION-DMA may be desorbed at high pH. The desorption experiments were performed at pH 11. We found that the desorption process could reach equilibrium within 90 min (see Figure S4 in the Supporting Information). To our delight, the adsorption capacity decreased not more than 16% after five cycles of desorption−adsorption compared with the original adsorption capacity (Figure 6d). On the basis of its excellent adsorption performance and convenient magnetic separation, the MION-DMA can be employed as an efficient adsorbent for environmental cleanup.

Catalysis. Inorganic nanocatalysts that can combine high catalytic efficiency with facile magnetic separation are highly desired for advanced catalysis applications. To demonstrate the versatility of the MIONs, in situ growth of Pt nanocatalysts on the surface of MION-DMA was studied. Because the MION-DMA possesses numerous amine groups, it can adsorb $PtCl_4^{2-}$ onto its surface by strong electrostatic attraction between amine group and $PtCl_4^{2-}$. Subsequent chemical reduction by $NaBH_4$ yields zerovalent Pt nanoparticles that anchored on the surface MION-DMA. The morphology of the resulted MION-Pt magnetic nanocatalysts was observed by TEM as shown in Figure 7a. The Pt nanoparticles with spherical shape and an average diameter of 3 ± 1 nm are well-distributed on the surface of MIONs. This observation indicates that the MION-DMA can serve as an efficient platform to first adsorb noble metal ions and then stabilize the as-prepared noble metal nanoparticles. The corresponding energy disperse spectroscopy (EDS) confirmed the existence of Pt in the MION-Pt sample (Figure 7b). The content of Pt according to the EDS result is 0.126 mmol/g. Similarly, the content of Pt in the MION-Pt determined by inductively coupled plasma mass spectrometry (ICP-MS, Agilent 7500cx) is 0.131 mmol/g.

To investigate the catalytic activity of the as-prepared MION-Pt nanocatalysts, reduction of 4-nitrophenol in the presence of $NaBH_4$ performed. This classic reaction has been widely employed to evaluate the catalytic efficiencies of noble metal nanocatalysts.[38−40] The reduction process was monitored by measuring the UV−vis spectra at different time as shown in Figure 7c. In the absence of MION-Pt, the reduction reaction does not proceed even in a large excess of $NaBH_4$, as evidenced by the fact that the peak at 400 nm ascribed to 4-nitrophenol remains unaltered. However, when MION-Pt nanocatalysts were introduced into the solution, the peak at 400 nm decreases and a new peak at 295 nm increases gradually, indicating the reduction of 4-nitrophenol and formation of 4-aminophenol, respectively. Seen from the sample solution, the bright yellow solution gradually becomes colorless after the addition of MION-Pt for about 5 min, indicating the complete reduction of 4-nitrophenol. Furthermore, we found that the MION-Pt could still exhibit high catalytic activity even after ten consecutive cycles of magnetic separation-reduction (Figure 7d). This excellent catalytic stability of MION-Pt is due to the presence of multiple amine groups that can tightly anchor the Pt nanoparticles. Therefore, our MIONs can be used as a versatile support to directly grow noble metal nanocatalysts on their surface.

4. CONCLUSION

In summary, we have demonstrated a one-step approach for large-scale synthesis of amine- and vinyl-capped MIONs by using vinyl-based tertiary amine molecules as both alkaline source and ligands. The as-prepared MIONs with an average diameter below 10 nm show good superparamagnetic performance and high dispersibility both in aqueous solution and organic solvents. The numerous vinyl groups on the surface of MIONs can be utilized to graft various polyvinyl-based polymers as exemplified by the in situ grafting PMMA in this study. On the basis of their numerous amine groups, the MIONs can not only work as a magnetic adsorbent with high adsorption capacity and rapid adsorption rate for anionic dye but also can serve as a catalyst support for in situ growth of noble metal nanoparticles with high catalytic efficiency. The MIONs show good reusability both for adsorption and catalysis applications. The concept of using functional vinyl-based amine molecules as ligands can also be extended to synthesize other metal oxide nanoparticles. This study not only presents a promising strategy for fabrication of versatile MIONs but also contributes to the understanding and design of inorganic nanoparticles with desired properties.

■ ASSOCIATED CONTENT

Ⓢ Supporting Information

TEM image of MION-$NH_3{\cdot}H_2O$, detailed adsorption isotherm studies, and desorption monitoring. This material is available free of charge via the Internet at http://pubs.acs.org.

■ AUTHOR INFORMATION

Corresponding Author

*E-mail: zhouli@glut.edu.cn.

Notes

The authors declare no competing financial interest.

■ ACKNOWLEDGMENTS

The authors appreciate financial support from the National Natural Science Foundation of China (No. 51103028 and No. 21364003), Guangxi Natural Science Foundation (No. 2012GXNSFBA053152), Foundation KH2012YB006, Guangxi Funds for Specially appointed Expert, and Guangxi Small Highland Innovation Team of Talents in Colleges and Universities.

■ REFERENCES

(1) Ho, D.; Sun, X. L.; Sun, S. H. *Acc. Chem. Res.* **2011**, *44*, 875−882.
(2) Lee, N.; Hyeon, T. *Chem. Soc. Rev.* **2012**, *41*, 2575−2589.
(3) Frey, N. A.; Peng, S.; Cheng, K.; Sun, S. H. *Chem. Soc. Rev.* **2009**, *38*, 2532−2542.
(4) Laurent, S.; Forge, D.; Port, M.; Roch, A.; Robic, C.; Elst, L. V.; Muller, R. N. *Chem. Rev.* **2008**, *108*, 2064−2110.
(5) Reddy, L. H.; Arias, J. L.; Nicolas, J.; Couvreur, P. *Chem. Rev.* **2012**, *112*, 5818−5878.

(6) Sun, S. H.; Zeng, H. *J. Am. Chem. Soc.* **2002**, *124*, 8204−8205.
(7) Rockenberger, J.; Scher, E. C.; Alivisatos, P. A. *J. Am. Chem. Soc.* **1999**, *121*, 11595−11596.
(8) Xu, Z. C.; Shen, C. M.; Hou, Y. L.; Gao, H. J.; Sun, S. H. *Chem. Mater.* **2009**, *21*, 1778−1780.
(9) Park, J.; Lee, E.; Hwang, N. M.; Kang, M.; Kim, S. C.; Hwang, Y.; Park, J. G.; Noh, H. J.; Kim, J. Y.; Park, J. H.; Hyeon, T. *Angew. Chem., Int. Ed.* **2005**, *44*, 2872−2877.
(10) Cheon, J.; Kang, N. J.; Lee, S. M.; Lee, J. H.; Yoon, J. H.; Oh, S. J. *J. Am. Chem. Soc.* **2004**, *126*, 1950−1951.
(11) Roca, A. G.; Marco, J. F.; Morales, M. P.; Serna, C. J. *J. Phys. Chem. C* **2007**, *111*, 18577−18584.
(12) Huang, S.; Yan, W.; Hu, G. F.; Wang, L. Y. *J. Phys. Chem. C* **2012**, *116*, 20558−20563.
(13) Amiri, H.; Mahmoudi, M.; Lascialfari, A. *Nanoscale* **2011**, *3*, 1022−1030.
(14) Sun, X. H.; Zheng, C. M.; Zhang, F. X.; Li, L. D.; Yang, Y. L.; Wu, G. J.; Guan, N. J. *J. Phys. Chem. C* **2008**, *112*, 17148−17155.
(15) Sun, X. H.; Zheng, C. M.; Zhang, F. X.; Yang, Y. L.; Wu, G. J.; Yu, A. M.; Guan, N. J. *J. Phys. Chem. C* **2009**, *113*, 16002−16008.
(16) Dassenoy, F.; Casanove, M. J.; Lecante, P.; Verelst, M.; Snoeck, E.; Mosset, A.; Ely, T. O.; Amiens, C.; Chaudret, B. *J. Chem. Phys.* **2000**, *112*, 8137−8145.
(17) Xu, C. B.; Teja, A. S. *J. Supercrit. Fluids* **2008**, *44*, 85−91.
(18) Ge, J.; Hu, Y.; Biasini, M.; Dong, C.; Guo, J.; Beyermann, W.; Yin, Y. *Chem.—Eur. J.* **2007**, *13*, 7153−7161.
(19) Zhou, L.; Gao, C.; Hu, X. Z.; Xu, W. J. *Chem. Mater.* **2011**, *23*, 1461−1470.
(20) Kim, P.; Doss, N. M.; Tillotson, J. P.; Hotchkiss, P. J.; Pan, M. J.; Marder, S. R.; Li, J.; Calame, J. P. *J. W. ACS Nano* **2009**, *3*, 2581−2592.
(21) Zhu, J.; Wei, S.; Ryu, J.; Budhathoki, M.; Liang, G.; Guo, Z. *J. Mater. Chem.* **2010**, *20*, 4937−4948.
(22) Zhu, J.; Wei, S.; Ryu, J.; Sun, L.; Luo, Z.; Guo, Z. *ACS Appl. Mater. Interfaces* **2010**, *2*, 2100−2107.
(23) Zhu, J. H.; Wei, S. Y.; Li, Y. T.; Sun, L. Y.; Haldolaarachchige, N.; Young, D. P.; Southworth, C.; Khasanov, A.; Luo, Z. P.; Guo, Z. H. *Macromolecules* **2011**, *44*, 4382−4391.
(24) Nata, I. F.; El-Safory, N. S.; Lee, C. K. *ACS Appl. Mater. Interfaces* **2011**, *3*, 3342−3349.
(25) Tao, K.; Dou, H. J.; Sun, K. *Chem. Mater.* **2006**, *18*, 5273−5278.
(26) Xin, X. D.; Wei, Q.; Yang, J.; Yan, L. G.; Feng, R.; Chen, G. D.; Du, B.; Li, H. *Chem. Eng. J.* **2012**, *184*, 132−140.
(27) Daou, T. J.; Pourroy, G.; Bégin-Colin, S.; Grenèche, J. M.; Ulhaq-Bouillet, C.; Legaré, P.; Bernhardt, P.; Leuvrey, C.; Rogez, G. *Chem. Mater.* **2006**, *18*, 4399−4404.
(28) Yu, W. W.; Falkner, J. C.; Yavuz, C. T.; Colvin, V. L. *Chem. Commun.* **2004**, 2306−2307.
(29) Xie, J.; Xu, C. J.; Xu, Z. C.; Hou, Y. L.; Young, K. L.; Wang, S. X.; Pourmand, N.; Sun, S. H. *Chem. Mater.* **2006**, *18*, 5401−5403.
(30) Depan, D.; Misra, R. D. K. *Nanoscale* **2012**, *4*, 6325−6335.
(31) He, H. K.; Zhang, Y.; Gao, C.; Wu, J. Y. *Chem. Commun.* **2009**, *13*, 1655−1657.
(32) Al-Ghouti, M. A.; Khraisheh, M.; Allen, S. J.; Ahmad, M. N. *J. Environ. Manage.* **2003**, *69*, 229−238.
(33) Qu, S.; Huang, F.; Yu, S. N.; Chen, G.; Kong, J. L. *J. Hazard. Mater.* **2008**, *160*, 643−647.
(34) Rocher, V.; Siaugue, J. M.; Gabuil, V.; Bee, A. *Water Res.* **2008**, *42*, 1290−1298.
(35) Zhou, L.; Gao, C.; Xu, W. J. *ACS Appl. Mater. Interfaces* **2010**, *2*, 1483−1491.
(36) Lorenc-Grabowska, E.; Gryglewicz, G. *Dyes Pigm.* **2007**, *74*, 34−40.
(37) Xia, C.; Jing, Y.; Jia, Y.; Yue, D.; Ma, J.; Yin, X. *Desalination* **2011**, *265*, 81−87.
(38) Huang, T.; Meng, F.; Qi, L. M. *J. Phys. Chem. C* **2009**, *113*, 13636−13642.
(39) Ge, J. P.; Huynh, T.; Hu, Y. P.; Yin, Y. D. *Nano Lett.* **2008**, *8*, 931−934.
(40) Zhou, L.; Gao, C.; Xu, W. J. *Langmuir* **2010**, *26*, 11217−11225.